

Imaging Protein States in Cells

Hernan E. Grecco and Philippe I. H. Bastiaens

*Department of Systemic Cell Biology, Max Planck Institute of Molecular Physiology,
Otto-Hahn-Strasse 11, 44227 Dortmund, Germany*

TO UNDERSTAND INTRACELLULAR SIGNALING, IT IS necessary to unravel how response dynamics emerges from the structure of the underlying biochemical network (Pieroni et al. 2008; Zamir and Bastiaens 2008). The description of the system in terms of a network (rather than many pathways) emphasizes the complex interrelationships that are needed to achieve the plethora of cellular responses. Proteins are the main building blocks of signaling networks, and their interactions provide the central links that define the architecture of these networks. Identifying the components and determining their interactions is thus the first step in a strategy to reverse-engineer network structure. Posttranslational modifications (PTMs) such as phosphorylation and ubiquitination modulate protein interactions and thereby enable the network to respond to input signals. It is therefore important not only to identify the proteins involved in signaling networks but also to determine their modification state.

Spatiotemporal regulation is an important aspect of signal transduction (Kholodenko 2006). For example, it has been shown that epidermal growth factor (EGF) and nerve growth factor (NGF) are both signals that operate through the mitogen-activated protein kinase (MAPK) pathway, but they lead to significantly different cell responses (proliferation versus differentiation [Santos et al. 2007]). Signal specificity is encoded in the temporal profile of MAPK activation, which is transient for EGF and sustained for NGF. This difference in response originates from input-context-dependent wiring of the MAPK-network module. In cell migration, the same network constituents result in advance or retraction, depending on the context of the local environment.

It is important to point out that although the discovery of connectivity (direct or indirect) between components is a necessary step, it does not by itself provide enough information to explain even simple regulated responses. The causality of the relations (i.e., the strength and sign of the interactions) must be incorporated into the description (Zamir and Bastiaens 2008). A common feature of almost all signaling networks is the presence of feedback loops (Csete and Doyle 2002; Milo et al. 2002; Tyson et al. 2003; Zhu et al. 2007). An aspect of this network motif is that the response of any given protein within a feedback loop contains information about the dynamics of the network as a whole. Each protein can be considered as an embedded probe that relays the coherent response of the network. Therefore, experiments on protein reactions within intact cells provide unsurpassed information as they explore logical connectivity including spatiotemporal constraints.

Functional microscopic imaging is thus a key tool for studying signaling because it provides simultaneous spatial and temporal information on protein-network behavior in intact cells (Bastiaens and Squire 1999; Vermeer and Bastiaens 2008). A dynamic topographic map of proteins in the cell should be combined with topologic information on the underlying network and

its state, consisting of population evolution of the different interacting or modified proteins.

However, protein interactions occur on such a short length scale that it is challenging for most microscopy techniques to distinguish between colocalization and physical interaction. To overcome this difficulty, fluorescence resonance energy transfer (FRET) microscopy and fluorescence cross-correlation spectroscopy (FCCS) were developed, and their utilization has gained momentum in the last decade as a result of the increased availability of genetically encoded biosensors and improved instrumentation. This chapter describes these microscopy-based approaches for quantifying protein interactions and posttranslational modifications in cells.

COLOCALIZATION VERSUS INTERACTION

The localization of proteins in the cell can be imaged using dye-labeled antibodies or by expressing fluorescent protein chimeras (Giepmans et al. 2006). Simultaneous imaging of two or more labeled species can be combined to investigate interactions and PTMs (Bolte and Cordelieres 2006; French et al. 2008). However, the fact that the images of the different molecules show colocalization in the same pixel does not imply that they are interacting. Because of the diffraction limit, a microscope is an optical low-pass filter, converting pointlike light sources in the sample into blurred images in the detector (Heintzmann and Ficz 2007). Molecules far away from each other (in the interaction sense) might appear together in the image, yielding false positive signals. It is then important to define what far away means by comparing the interaction scale (typically a few nanometers) with the measurement scale, which depends on the illumination and detection optics as well as on the photophysical phenomena being used as a probe.

The most common microscopy techniques are shown schematically in Figure 1. In wide-field (Fig. 1A) and confocal microscopy (Fig. 1B), the area of observation in the focal plane is mainly defined by the numerical aperture of the system. The main difference stands in the resolution in

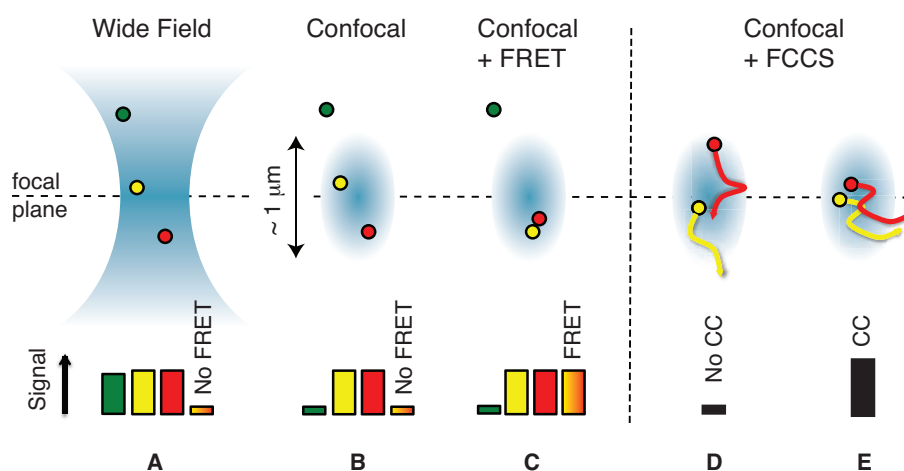


FIGURE 1. Comparison of different microscopy schemes and their readouts to study protein interactions. The detection volume is represented in blue, and three dots (green, yellow, and red) represent the proteins being studied. (A) In wide-field microscopy, the detection volume extends along the axial direction yielding a significant signal for molecules even away from the focal plane. (B) In confocal microscopy, light coming from out-of-focus particles (green) is rejected. However, because of the size of the confocal volume, two noninteracting particles will appear as colocalizing. Contrary to this, the steep nanometer distance dependence of (C) FRET will only yield a positive signal when particles interact. (D,E) In FCCS, particles in the complex will diffuse together through the confocal volume resulting in a high coincidence of the intensity traces and therefore a high cross-correlation amplitude.

the optical axis: Confocal microscopy rejects out-of-focus light, whereas wide-field microscopy does not. The resulting effect is that signals from the three particles illustrated will colocalize in wide-field microscopy, but only the yellow and red will do so in confocal microscopy. The confocal volume ($\sim 1 \mu\text{m}^3 = 1 \text{ fL}$) is still much larger than the interaction range. Developments in light microscopy have provided different methods to break the diffraction limit (Betzig et al. 2006; Medda et al. 2007; Hein et al. 2008) with good results. However, their use in biology is still limited, especially in highly dynamic systems such as live cells. Two methods to overcome this difficulty will be discussed in the following sections: FRET, which is based on a photophysical interaction with a length scale much shorter than the confocal volume (Fig. 1C), and FCCS, which makes use of the fact that two particles that interact will codiffuse through the confocal volume and thus yield highly similar photon coincidence time traces (Fig. 1D).

FRET

When two fluorophores are in close proximity, excitation energy can be nonradiatively transferred as a result of dipole–dipole coupling (Forster 1948; Lakowicz 2006). Energy flows from the excited donor fluorophore to an acceptor fluorophore with an efficiency defined by

$$E = \frac{1}{1 + (r/R_0)^6}, \quad (1)$$

where r is the distance between the fluorophores and R_0 is the distance at which 50% of the excitation energy is transferred. This value is dependent on the photophysical properties of the fluorophore pair. When choosing a good FRET pair, it is important that a substantial overlap exists between the emission spectra of the donor and the absorption spectra of the acceptor as depicted in Figure 2. For most biologically relevant FRET fluorophore pairs, the value of R_0 is around 5 nm (Patterson et al. 2000), yielding a sensing volume of 10^{-7} fL , seven orders of magnitude smaller than the confocal volume. It is important to emphasize that the detection of FRET does not increase the resolution of the system but provides a sensor with a discrimination length appropriate to distinguish between interacting and noninteracting molecules within a spatially resolvable volume element of the optical system.

In the experimental protocols included in this chapter, we describe how to measure the spatiotemporal profile of EGF receptor (EGFR) phosphorylation upon stimulation (Verveer et al. 2000; Haj et al. 2002) using FRET imaging. The receptor is fused to a fluorescent protein acting as the donor, and the acceptor is an organic dye conjugated to an antibody directed against phosphotyrosine (PY72). It is important to note that if FRET is measured via a change in the donor photophysical properties (such as fluorescence lifetime), the antibody does not need to uniquely recognize the epitope on the donor-tagged protein. Signal specificity is achieved because of the reduced detection volume of FRET. Protocols 1 and 2 provide instructions for labeling such an antibody and preparing the cells for FRET analysis. On excitation of the donor, FRET can be observed by (1) quenched donor emission, (2) increased sensitized acceptor emission, and (3) the decrease of the fluorescence lifetime of the donor. In the following sections, an explanation for each method is given, and Protocols 3 and 4 provide the corresponding instructions for performing experiments.

FRET Quantification by Donor Quenching

Upon excitation of the donor, a fraction E of the excitation energy is not emitted by donor fluorescence but instead transferred to the acceptor that is in close proximity. This leads to a decrease in the donor intensity proportional to the number of donor molecules in close proximity to an acceptor within the detection volume. A straightforward method to quantify FRET is to compare

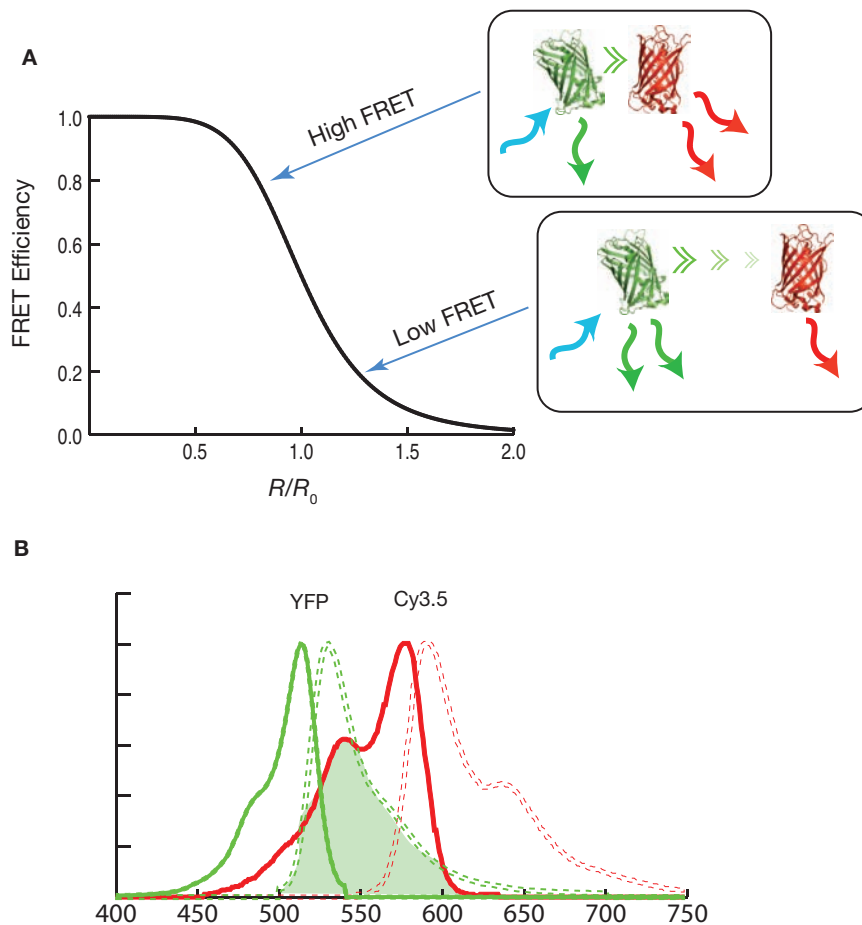


FIGURE 2. (A) The energy-transfer efficiency from donor to acceptor is a steep function of their relative distance. When donor and acceptor are in close proximity, energy is transferred efficiently, resulting in a quenched emission of the donor and sensitized emission of the acceptor. The distance at which 50% of the excitation energy is transferred is called Förster distance and depends on the photophysical properties and relative orientation of the FRET pair. (B) The spectral overlap (shaded in green) between the normalized emission spectra (dashed green) of the YFP (donor) and the normalized excitation (solid red) of the Cy3.5 (acceptor).

the quenched and unquenched emissions of the donor (Bastiaens and Jovin 1996; Wouters et al. 2001). This can be accomplished experimentally by imaging the specimen before ($I_D[x, y]$) and after photobleaching the acceptor ($I_D^{\text{apb}}[x, y]$) (see Fig. 3). The apparent FRET efficiency, defined as the true FRET efficiency multiplied by the fraction of donor molecules in close proximity to an acceptor (α), can be calculated pixel by pixel from the acquired images as

$$\frac{I_D^{\text{apb}} - I_D}{I_D^{\text{apb}}} = E \frac{[\text{DA}]}{[\text{D}] + [\text{DA}]} = E\alpha, \quad (2)$$

where $[\text{DA}]$ is the number of donor molecules in close proximity to an acceptor and $[\text{D}] + [\text{DA}]$ is the total number of donor molecules, and therefore its ratio yields α . The dependence on (x, y) has been dropped for clarity. If the transferred efficiency E is assumed spatially invariant, then the biologically relevant information is contained solely in α .

In the study on the phosphorylation of EGFR described here, α corresponds to the molar fraction of the phosphorylated receptor as measured by the fraction of the receptor that is bound to the antibody. However, without the knowledge of the true FRET efficiency in the complex, the appar-

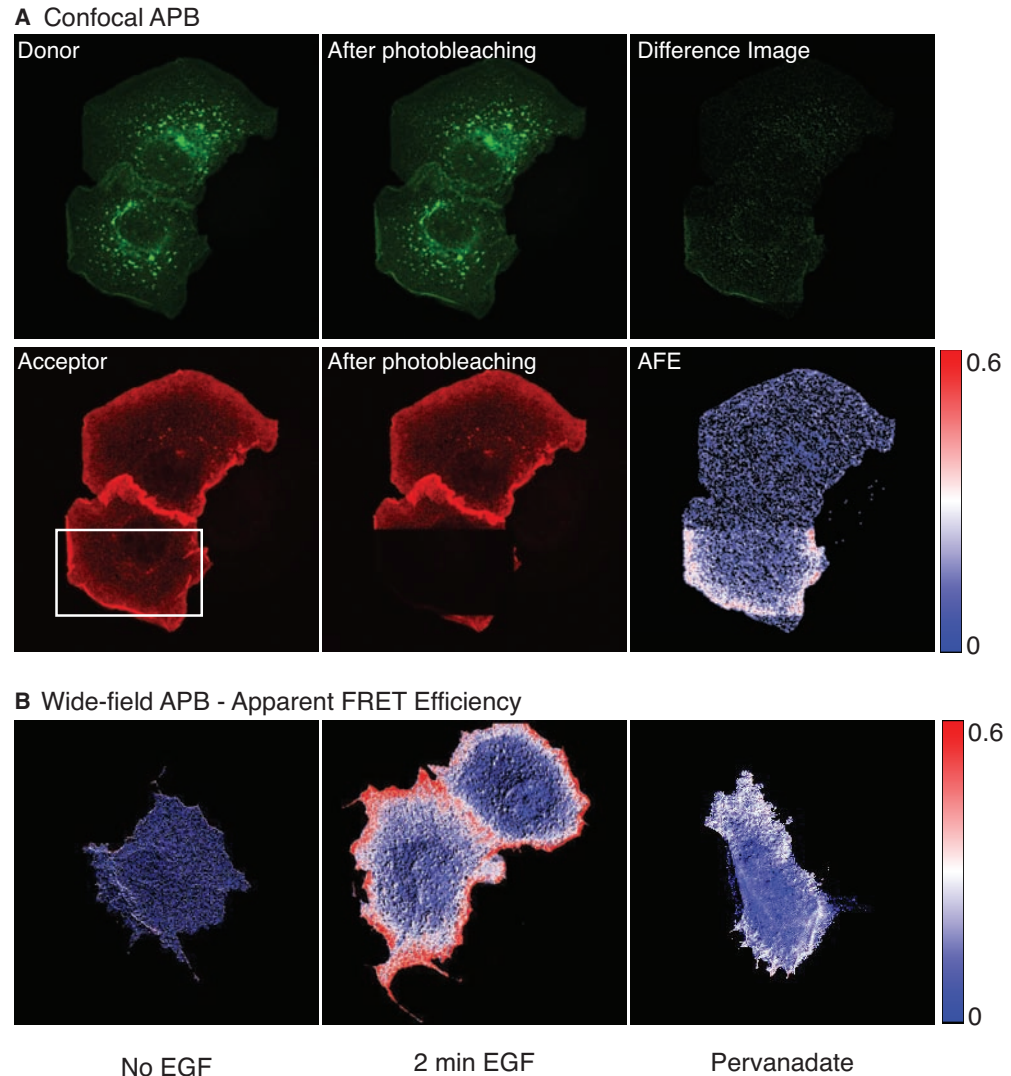


FIGURE 3. Measuring the phosphorylation of the EGFR using acceptor photobleaching (APB). (A) Example of confocal APB. After bleaching the acceptor, donor intensity and apparent fluorescence resonance energy-transfer efficiency (AFE) increase in the membrane where the donor and acceptor are in complex. (B) Example of wide-field APB. Without EGF, the receptor shows a negligible and uniform phosphorylation as evidenced from the AFE. Upon addition of the growth factor, the phosphorylation increases in the periphery. After treatment with sodium pervanadate, a generic phosphatase inhibitor, phosphorylation levels increase ubiquitously.

ent FRET efficiency (or better called the apparent bound fraction) is an underestimation of the real bound fraction α and can only be quantitatively used as a relative indicator. Moreover, because $E \leq 1$, small differences in α will lead to even smaller differences in the apparent FRET efficiency. The importance of having a good FRET pair is again clear, as the dynamic range of the measurement will be dependent on it. Because of the possible diffusion of donor molecules during the time required for photobleaching (1–30 min), this method is better suited for fixed cells. In Protocol 3, a practical example of this technique is given together with a more detailed explanation of image processing.

FRET Quantification by Sensitized Emission of the Acceptor

Measuring the emission of the acceptor upon donor excitation (I_{DA}) is also a straightforward method to quantify FRET (Mahajan et al. 1998). However, experimentally this is a more complex

situation than acceptor photobleaching because the detected signal is contaminated by photons that do not come from sensitized emission. Indeed, some donor-emitted photons will bleed through into the acceptor channel, as most emission spectra have long tails toward the red. Conversely, the acceptor is directly excited, as excitation spectra tend to expand toward the blue. The real contribution of sensitized emission can be obtained by performing spectral unmixing. By obtaining for the same sample an acceptor image upon acceptor excitation (I_A) and a donor image upon donor excitation (I_D), bleed through and direct excitation can be subtracted from I_{DA} . The resulting image normalized by I_A is proportional to the apparent FRET efficiency:

$$\frac{I_{DA} - B \cdot I_D - C \cdot I_A}{I_A} = FE \frac{[DA]}{[A] + [DA]} = FE\alpha_A, \quad (3)$$

where F is the ratio between the donor and acceptor brightness; B is a scalar bleed-through factor, which can be obtained from a sample containing only a donor by dividing the total intensity in the FRET channel by the total intensity in the donor channel; and C is a scalar direct-excitation factor that can be obtained from a sample containing only an acceptor by dividing the total intensity in the FRET channel by the total intensity in the acceptor channel. These correction factors can also be obtained from regions of the doubly labeled sample in which only one of the fluorophores is present.

This technique is especially appropriate for live cell imaging of relatively fast physiological processes, as it does not require any long acquisition step such as bleaching. Notice, however, that the result yields a value that is proportional to the fraction of acceptor in a complex instead of the fraction of donor in a complex as described for acceptor photobleaching. This can be problematic when there is an excess of acceptor in the sample, as this will yield very low values.

As discussed above, intensity-based approaches only provide relative information about the fraction of molecules in which FRET occurs. Although independent experiments could be done to estimate the unknown parameters (E and F), their sensitivity to environmental conditions makes this undesirable. Therefore, to obtain the absolute value for the fraction of molecules in which FRET occurs in a robust way, the true FRET efficiency should be obtained simultaneously. Fluorescence lifetime measurements provide a way to do this.

FRET Quantified by Fluorescence Lifetime Imaging

After being excited by light, a molecule spends a certain amount of time in the excited state before returning to the ground state via radiative (emitting a photon) or nonradiative (e.g., vibrational) decays. The average time the molecule spends in the excited state before emitting a photon is called fluorescence lifetime and is typically on the order of a few nanoseconds (10^{-9} sec) for most chromophores used in biology. The quantum yield (QY), defined as the number of photons emitted normalized by the number of photons absorbed, expresses from 0 to 1 the competition between radiative and nonradiative processes. QY can be explicitly formulated as the ratio between fluorescence lifetime (τ) and the fluorescence lifetime in the absence of nonradiative processes (τ_R) (Lakowicz 2006):

$$QY = \frac{\tau}{\tau_R}. \quad (4)$$

When FRET takes place between donor and acceptor, the donor is quenched, and thus its QY is reduced. The fluorescence lifetime is a direct measurement of the QY, and it can therefore be used to quantify FRET.

Two equivalent approaches, named time-domain (Lakowicz et al. 1987; Dowling et al. 1998) and frequency-domain (Lakowicz and Berndt 1991; Gadella et al. 1993; Bastiaens and Squire 1999), are used to obtain fluorescence lifetime data. Here we describe the former, which constitutes an easy-to-understand and straightforward measurement of the fluorescence-decay profile

EGFR-YFP and PY72-Cy3.5

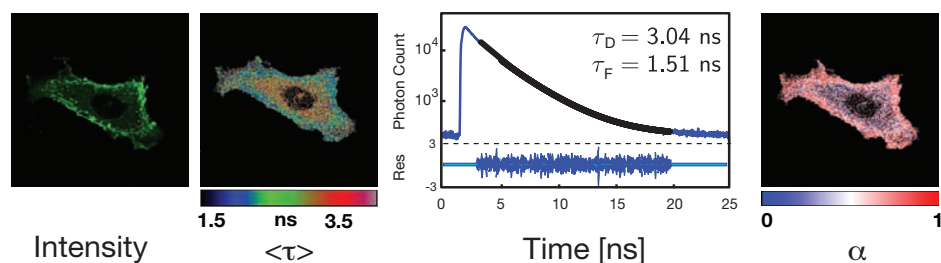


FIGURE 4. Measuring the phosphorylation of EGFR using confocal FLIM. Upon excitation with a pulse, molecules are pumped to the excited state and decay with two distinct fluorescence lifetime values corresponding to the free and acceptor-bound donor molecules. The local presence of FRET is evidenced by a drop in the mean value of the fluorescent lifetime, the value of which can be calculated pixel by pixel. A quantitative determination of the fraction of the donor in the complex with the acceptor can be made by fitting the fluorescence decay profile integrated over the whole image with two exponential functions corresponding to donor and donor-in-complex decay profiles. The spatially variant fraction of the donor-in-complex can be obtained by fitting the decay amplitudes in each pixel while keeping the fluorescence lifetimes fixed to the values obtained globally.

of a molecule. In this technique, the sample is illuminated with a pulsed light source, and the fluorescence emission is recorded as a function of time. The molecules are pumped to the excited state throughout the duration of the pulse, and the fluorescence decay profile as a function of time from the excitation pulse is directly measured afterward.

At each time point of the sample, different species with different fluorescence decay profiles might be present. The measured decay profile in each pixel is thus the sum of the different decay profiles scaled by their respective populations. On the assumption that the free donor molecules have a single fluorescence lifetime (τ_D) and that the acceptor molecules have a single spatial configuration relative to the donor in the complex (leading to a single reduced fluorescence lifetime of the donor; τ_F), the decay profile in each pixel is the sum of two populations plus an additive background term (BG) that account for the dark noise of the detector (Equation 5). These two populations with amplitudes A_D and A_F correspond to the free and acceptor-bound donor molecules:

$$I(x, y, t) = A_D(x, y)e^{-t/\tau_D} + A_F(x, y)e^{-t/\tau_F} + \text{BG}, \quad (5)$$

$$\alpha(x, y) = \frac{A_F(x, y)}{A_D(x, y) + A_F(x, y)}, \quad (6)$$

$$E = 1 - \frac{\tau_F}{\tau_D}, \quad (7)$$

where the coordinates (x, y) are explicitly shown to emphasize that interacting populations are varying within the object while the fluorescence lifetimes, and thus the FRET efficiency, are considered spatially invariant (only dependent on the spatial configuration of the protein complex). (See Fig. 4.)

FLUORESCENCE (CROSS-)CORRELATION SPECTROSCOPY

Fluorescence correlation spectroscopy (FCS) (Magde et al. 1972) is a powerful tool for measuring concentrations, diffusion coefficients, and molecular interactions in the intracellular domain (Sanchez and Gratton 2005; Kim et al. 2007). It is based on the fact that fluctuations of the fluorescence emitted by a molecule while diffusing through a confocal volume contain information about ongoing dynamic processes. Consider the simplest case in which diffusion is the only fluctuation source. Photons emitted from the same molecule will be correlated, whereas photons

emitted from different molecules will not be correlated. The autocorrelation function can be calculated from the fluctuations of the intensity time trace ($\delta I(t) = I(t) - \langle I(t) \rangle$) as

$$G(T) = \frac{\langle \delta I(t) \delta I(t+T) \rangle}{\langle I(t) \rangle^2}. \quad (8)$$

The duration of the correlation function is a direct measurement of the dwell time of the molecules in the confocal volume (T_d) and thus of the diffusion coefficient, if the volume shape is known.

The number of molecules within the confocal volume is governed by Poissonian statistics, and thus its variance and mean value are equal. The amplitude of the autocorrelation ($G[0]$), which is the ratio between the variance of the intensity and the square of mean intensity, is then inversely proportional to the mean number of fluorescent particles (N) in the confocal volume element. Therefore, low concentrations ($1-10^3$ nM) of fluorescent-tagged proteins should be used to obtain measurable amplitudes. It is important to point out that absolute calibration can only be obtained if proper calibration of the confocal volume is performed. The computed autocorrelation function can then be fitted by

$$G(T) = \frac{1}{N} \frac{1}{1+T/T_d} \sqrt{\frac{1}{1+T/(S^2 T_d)}}, \quad (9)$$

where S is the structural parameter representing the aspect ratio of the axial and lateral radii of the detection volume, which must be determined independently. Equation 9 only applies to single-diffusing species. More complex kinetics such as blinking, triplet formation, binding, or multiple species will require different fitting models (Haustein and Schwillie 2007).

In FCCS (Bacia et al. 2006), the fluorescent fluctuations of two different fluorescent species are tracked in two independent channels (usually named green and red), which are then cross-correlated. In the noninteracting case, the fluorescence fluctuations in the two channels will be uncorrelated. In contrast, if a complex is formed, the intensity fluctuation traces will be highly similar, as particles will codiffuse through the confocal volume. The concentration of interacting proteins (C_{rg}) can be calculated from the auto- and cross-correlation amplitudes and the volume overlap (V_{rg}):

$$C_{rg} = \frac{G_{rg}(0)}{G_{gg}(0) \cdot G_{rr}(0) \cdot V_{rg}}. \quad (10)$$

CONCLUSION

Spatiotemporally resolved quantitative determination of interactions and PTMs is needed to unravel the topology of signaling networks. FRET approaches provide a unique tool in terms of spatial resolution and specificity in which the biological relevant outcome is the fraction of donor-tagged molecules in the complex with the acceptor. FC(C)S provides the ability to obtain absolute concentrations of molecules and their complexes and to study fast physiological processes. However, in most current commercial instrumentations, FC(C)S is a point measurement lacking spatial resolution. Several attempts have been made to overcome this problem trading temporal resolution for spatial resolution, limiting the ability to study highly dynamic processes in cells (Brown et al. 2008). The combination of FRET and FCS provides a unique method to obtain absolute concentrations in spatially inhomogeneous systems. This concept has been recently used to study the spatial regulation of Fus3 MAPK activity in yeast pheromone signaling (Maeder et al. 2007).

PROTOCOL 1

Antibody Labeling with Fluorescent Dyes

The phosphorylation of EGFR can be studied by FRET using a chimeric fluorescent EGFR and a dye-labeled generic antiphosphotyrosine antibody (PY72). There are many suitable FRET pairs, and the protocols outlined here use either enhanced green fluorescent protein (EGFP) with Cy3 or enhanced yellow fluorescent protein (EYFP) with Cy3.5. The latter is desirable if fluorescence lifetime measurements are to be performed because the YFP fluorescence-decay profile can be characterized by a single fluorescence lifetime.

MATERIALS

CAUTION: See Appendix for proper handling of materials marked with <I>. See the end of the chapter for recipes for reagents marked with <R>.

Reagents

Conjugation buffer (bicine buffer; 1 M; pH 9)

Cy3 or Cy3.5 monofunctional sulfoindocyanine succinimide esters (GE Healthcare; PA23001 or PA23501)

Cy dyes are provided as lyophilized samples that must be maintained in a desiccated environment at all times because they react with water.

N,N-dimethylformamide (DMF; dry) <I> <R>

Phosphate-buffered saline (PBS) <R>

PY72 generic antiphosphotyrosine antibody (Santa Cruz Biotechnology; sc-57577)

Tris-Cl (100 mM, pH 8.0; or other free-amine-containing buffer) <R>

Equipment

Centrifuge (tabletop)

Protein-desalting spin column (Pierce, 89849)

Sodium dodecyl sulfate (SDS)-polyacrylamide gel electrophoresis equipment (see Step 9)

UV-visible absorption spectrophotometer

METHOD

1. Resuspend a single vial of lyophilized Cy dye in 20 μL of dry (water-free) DMF to make a Cy solution with a concentration of ~ 10 mM.
2. To calculate the dye concentration, dilute 1 μL of Cy solution 1:10,000 in PBS, and calculate the dye concentration from the visible peak absorption.
The extinction coefficient (ϵ) for Cy3 and Cy3.5 is $150 \text{ mM}^{-1} \text{ cm}^{-1}$ at 552 nm and 581 nm, respectively. The amount of dye in each vial must be quantified individually because batch variation can occur.
3. The dye solution is now ready for labeling the protein of interest. If the protein solution contains low-molecular-weight components (e.g., Tris or dithiothreitol [DTT]) that are not compatible with labeling, then replace with PBS.

4. Replace protein buffer with PBS on a protein-desalting spin column.
 - i. Equilibrate the column five times with 400 μL of PBS. Discard the flowthrough.
 - ii. Centrifuge at 1500g for 2 min to remove excess liquid.
 - iii. Load the protein onto the middle of the resin.
 - iv. Centrifuge at 1500g for 2 min.
 - v. Collect the flowthrough, which is the antibody in PBS.
5. Add a volume of 1 M bicine buffer (pH 9) to the protein sample that equals 1/10 of the sample volume to reach a final concentration of 0.1 M bicine.

It is necessary to maintain an alkaline pH in the labeling reaction (while preserving protein integrity) so as to promote deprotonation of ϵ -amino groups of lysine residues, which is needed for efficient coupling.
6. Incubate the antibody (typically in a 0.1–0.5-mL volume at 1–10 μM) with a 10- to 40-fold molar excess of dye for 30 min at room temperature. Add the dye very slowly with the pipette tip while simultaneously stirring the solution.

To avoid protein denaturation by DMF, the volume of Cy/DMF added must not exceed 10% of the total volume. The determination of the optimal molar excess and reaction time is ultimately empirical, such that the final labeling ratio (molecules of dye/molecules of protein) is between 1 and 6 dye molecules per protein molecule (see Step 10 below for labeling ratio criteria). This varies greatly with individual proteins or antibodies. The antibody can be relabeled if the final labeling ratio is too low.
7. Terminate the labeling reaction by adding a free-amine-containing buffer such as Tris-Cl (100 mM; pH 8.0) to a final concentration of 10 mM.
8. Remove the excess unreacted dye by exchanging the buffer on a protein-desalting spin column, and elute the protein into the buffer of choice (typically PBS).
 - i. Equilibrate the column five times with 400 μL of PBS (pH 7.4).
 - ii. Load the labeling reaction mixture directly onto the resin to maximize separation. Apply it to as small an area as possible.
 - iii. Centrifuge at 1500g for 2 min.
 - iv. Collect the flowthrough, which is the labeled antibody.
9. Verify covalent labeling of the protein by sodium dodecyl sulfate-polyacrylamide gel electrophoresis (SDS-PAGE). After electrophoresis of the sample, examine the gel directly on an ultraviolet transilluminator (302 nm). A fluorescent band should migrate at the expected molecular weight of the protein. There should be no fluorescence from free dye at the migration front. See *Troubleshooting*.
10. Measure the absorption at the protein peak (280 nm) and at the dye absorption peak. Calculate the labeling ratio (molecules of dye/molecules of protein) using the formula

$$\frac{A_{\lambda} M}{(A_{280} - A_{\lambda} f) \epsilon(\lambda)},$$

where A_{λ} is the absorption of the dye at its absorption maximum at wavelength λ , A_{280} is the absorption of the protein at 280 nm, M is the molecular mass of the protein in kDa, and $\epsilon(\lambda)$ is the molar extinction coefficient of the dye at wavelength λ in $\text{mM}^{-1} \text{cm}^{-1}$. The equation also corrects for absorption of the dye at 280 nm. The factor f is the ratio between absorption of the dye at 280 nm and its maximal visible absorption at wavelength λ . The values of these parameters are available in the product information sheet.

See *Troubleshooting*.

TROUBLESHOOTING

Problem (Step 9): No bands are visible upon gel illumination after the labeling reaction.

Solution: Ultraviolet excitation at 302 nm is suboptimal for most dyes. Consider excitation at a different wavelength.

Problem (Step 10): Labeling ratio is low.

Solution: Make sure that the DMF is dry because water reacts with succinimide esters. Perform the labeling reaction in a buffer free of amine groups; for example, avoid Tris. Many commercial antibody preparations are provided with stabilizing agents that contain free-amino groups (such as bovine serum albumin [BSA] or gelatin) that will compete for the Cy dye. A number of suppliers will provide the antibody preparations free of these compounds upon request. In this case, request that they be provided at 1 mg/mL in PBS. Note that reducing agents such as DTT or β -mercaptoethanol will also interfere with the labeling reaction. If a reducing agent must be included to maintain biological/protein function, β -mercaptoethanol has a lower interference than DTT.

► PROTOCOL 2

Preparation of Cells for FRET Analysis

In this experiment, the human breast cancer cell line MCF7 is transfected with plasmids encoding the human EGFR (systematic name ErbB1) fused at its carboxyl terminus to EGFP or EYFP. After stimulation with EGF or sodium pervanadate, cells are fixed, permeabilized, and mounted for microscopy.

MATERIALS

CAUTION: See Appendix for proper handling of materials marked with <!>. See the end of the chapter for recipes for reagents marked with <R>.

Reagents

Activated sodium orthovanadate <!> <R>
BSA
EGF
Growth medium (Sigma Dulbecco's modified Eagle's medium [DMEM] containing 10% FCS [tested to support MCF7 growth] and glutamine/penicillin/streptomycin)
MCF7 cell line
Mowiol mounting medium <R>
Paraformaldehyde fixative solution (4%) <R>
PBS <R>
Plasmid DNA (pEGFP-ErbB1 or pEYFP-ErbB1)
Starvation medium (Sigma DMEM containing 0.1% FCS [tested to support MCF7 growth] and glutamine/penicillin/streptomycin)
Transfection reagent (e.g., FuGENE 6; Roche Applied Science)
Tris (50 mM; pH 8.0), containing 100 mM NaCl
Triton X-100 <!>
Trypsin/EDTA (e.g., PAN P10-023100SP)

Equipment

Coverslips (18-mm; washed and sterilized with ethanol)
Jeweler's forceps
T75 flasks
Tissue culture plates (six-well)

METHOD

Previous Week

1. Place 18-mm coverslips into each well of a six-well plate.

Day -3 (Evening)

2. Wash MCF7 cells growing in T75 flasks (should be grown to a density of 70%–90%) with 5 mL of PBS, and add 2 mL of trypsin/EDTA. After 2 min, add 8 mL of growth medium, and

triturate by pipetting up and down 10 times. Plate 200,000 cells per well of the six-well plate containing the sterile coverslips.

Day -2 (Evening)

3. Prepare the transfection complex by mixing 582 μL of DMEM and 18 μL of FuGENE 6.
Avoid unnecessary contact of the reagent with plastic surfaces. Add the reagent directly into the DMEM. FuGENE 6 is highly volatile. Avoid delays during pipetting or after opening the stock vial.
4. Vortex for 1 sec, or flick the tube to mix. Incubate for 5 min.
5. Add 6 μg of DNA. Limit the total volume added to 3–300 μL .
6. Vortex for 1 sec, or flick the tube to mix.
7. Incubate the mix for 15 min at room temperature.
8. Add 100 μL of transfection mixture to each well of the six-well plate.

Day -1

9. Prewarm the starvation medium in a water bath at 37°C. Replace the growth medium in each well with 1 mL of starvation medium.
10. After 4 h, prepare two stimulation media: (i) starvation medium containing 100 ng/mL EGF and (ii) starvation medium containing 1 mM activated orthovanadate. Replace the starvation medium with the stimulation medium. Add EGF-containing medium to wells 2–5 and pervanadate-containing medium to well 6. Well 1 is the untreated control. Start the timer immediately.
11. Fix the cells at exactly the following time points: well 2, 1 min; well 3, 5 min; well 4, 15 min; wells 1, 5, and 6, 30 min. Fix the cells by quickly rinsing them with 2 mL of prewarmed (37°C) PBS for 1–2 sec immediately followed by transfer to a six-well plate containing 2 mL of prewarmed 4% paraformaldehyde fixative solution.
Paraformaldehyde is the fixative of choice when performing FRET experiments because it is a cross-linking agent that preserves the integrity of protein interactions and (unlike methanol) does not precipitate cellular proteins.
12. After 10 min, quickly wash the cells with 50 mM Tris (pH 8.0) containing 100 mM NaCl to rinse off excess fixative. Repeat wash for 5 min to quench the remaining aldehyde groups.
13. Permeabilize cells with 2 mL of 0.1% Triton X-100 in PBS (pH 7.4) for 15 min.
14. Wash the cells three times with PBS (two quick rinses and one 5-min wash).
15. Block the cells with 2 mL of 5% BSA in PBS (pH 7.4) for 30 min.
16. Stain the cells with 25 μL of Cy3-labeled PY72 antibody (diluted in 1% BSA/PBS at 10 $\mu\text{g}/\text{mL}$) for 45 min. To do this, add 25 μL of the antibody onto parafilm in a humidified chamber; flip the coverslip cell-side down onto the drop. After incubation, add a 100- μL droplet of PBS on the edge of the coverslip. This will raise the coverslip sufficiently to allow you to grasp the edge with jeweler's forceps. Carefully lift up coverslips with forceps, place them back into the six-well plate cell-side up, and wash five times with PBS.
17. Blot off excess PBS with a tissue at the edge of the coverslip. Do not allow the cells to dry out.
18. Mount the coverslips cell-side down on 10 μL of Mowiol upon glass microscope slides, and allow them to harden overnight at 4°C. Avoid formation of air bubbles. Use two coverslips per holder. The Mowiol must solidify before imaging. Do not use nail polish as this has been shown to quench GFP fluorescence.

► PROTOCOL 3

Measuring FRET by Acceptor Photobleaching

The following protocol gives instructions for performing acceptor photobleaching using either a wide-field or a confocal microscope. Using a confocal microscope makes it possible to perform the measurement in a region of interest (ROI) in which the acceptor is photobleached. The result can then be compared to regions in the same cell that are not photobleached. Wide-field microscopes do not allow the limiting of the region of irradiation to an arbitrary ROI. However, it is possible to use the field diaphragm to limit the illumination to the center of the image. Alternatively, acceptor destruction can be performed on the whole image.

IMAGE ACQUISITION AND IMAGE PROCESSING

To perform quantitative measurements using imaging techniques, it is imperative to understand the capabilities and limitations of the equipment being used and the basics of image processing. Although this is not the aim of this chapter (more information about this can be found in Chaps. 4, 7, 15, 16, and 18), some basic guidelines will be given. All image-processing steps described in this chapter can be performed with the free application ImageJ (Sheffield 2007), which can be downloaded from <http://rsb.info.nih.gov/ij/>.

Boost the Dynamic Range

In wide-field microscopes, adjust the exposure time so that the cells are clearly distinguishable from the background, and check that the maximum value is just below the saturation level of the camera. In samples in which bleaching is a problem, a compromise should be found. Cell-to-cell intensity might be very different because of different transfection efficiencies, and within one cell highly localized proteins might be very bright in some places but dim in others. Do not try to achieve perfect exposure for every pixel, but concentrate on regions of interest in the cells. In confocal microscopes, use the laser power, gain, and offset to achieve the same result. In addition, be sure that the background levels in the region without cells are above the underexposed value (usually 0). This will be important to characterize the background and to correct for it.

Avoid Stray Light

Any light not coming from the sample will reduce the dynamic range of your measurement. Minimize stray light by turning off all lights in the microscopy room or covering the sample.

Avoid Sample Movement

Movement of the stage or the sample will lead to artifacts when performing a pixel-by-pixel image processing calculation; take care to reduce it. Refocus if needed. If sample drift is unavoidable, lateral shift can be corrected using standard registration techniques. An example of one of these techniques based on image correlation is given below.

1. Calculate the Fourier transform of image 1 (I_1).
2. Calculate the Fourier transform of image 2 (I_2).

3. Multiply the conjugate of the Fourier transform of I_1 with the Fourier transform of I_2 .
4. Take the inverse Fourier transform of the result to get the correlation image.
5. Find the distance of the maximum in the correlation image from the center of the image. The shifts (Δx , Δy) between the images are equal to the horizontal and vertical distances between the peak and the origin of the image.
6. Shift I_2 accordingly.

Caution: This automated registering procedure requires that the content of the two images is reasonably similar or it may fail. Always check to see that the registration procedure is applicable for the application at hand, for example, by subtracting registered images and looking for shadows at the edges that indicate failure of the registration procedure.

Think Ahead

When comparing two images (e.g., as in acceptor photobleaching [APB] FRET) without further calibration, keep the acquisition parameters constant whenever possible. If the second image is expected to be brighter than the first, do not acquire the first image close to detection saturation.

Correct for Background

Calculations involving ratios between images will be biased by the presence of additive background. A correction can be applied performing the following steps.

1. Select a small region in the background. (Be sure that there are no dim cells present by changing the brightness and contrast of the image.)
2. Calculate the mean intensity in this region.
3. Subtract this mean intensity from the image.

Mathematical Operations on Pixels

Most image formats store the value for each pixel as 8- or 16-bit integers, leading to maximum values of 256 or 65,535, respectively. To avoid calculation artifacts due to the limitation of the container type, convert all images to real data types before performing any mathematical operations.

Threshold

Division by pixels that have a very low value will lead to noise amplifications. Therefore, all pixels in which the denominator is lower than an empirically chosen value should be ignored for calculations by setting them to not a number.

MATERIALS

Equipment

For wide-field acceptor photobleaching

Use a wide-field microscope equipped with a fluorescent lamp, digital camera, and filter sets to acquire donor and acceptor images. Any type of objective can be used. However, 40X or 60X magnification is suggested to appreciate the progression of EGF stimulation. High numerical aperture is desirable to maximize photon collection and to increase resolution.

For confocal acceptor photobleaching

Use a confocal microscope equipped with laser lines and filter sets to acquire donor and acceptor images. Any type of objective can be used. High numerical aperture is desirable to maximize photon collection and to increase resolution.

METHOD

1. Select a cell that exhibits donor and acceptor fluorescence. In all steps take care to minimize donor photobleaching.
2. Acquire an image with the donor filter set (I_D). Remember that after photobleaching the acceptor, the donor intensity is expected to increase; therefore, do not acquire the first image close to the detector saturation.
3. (*Optional*) Acquire an image with the acceptor-filter set (I_A) to document the distribution of the acceptor.
4. Photodestruct the acceptor in an ROI or in the whole image by continuous illumination with the acceptor-filter set until fluorescent signals are below background levels. The amount of time needed will depend on the acceptor photostability, concentration, and light power. Typical values are 30 min using a lamp illumination and 1 min using a laser at full power.
 Caution: Incomplete photodestruction will lead to an underestimation of apparent energy transfer.
5. Acquire a donor image (I_D^{apb}) as in Step 2.
6. (*Optional*) Acquire an image with the acceptor-filter set (I_A^{apb}) to document the photodestruction.
7. Perform background correction, and calculate the apparent energy-transfer efficiency in every pixel using Equation 2:

$$\text{AFE}_D = \frac{I_D^{\text{apb}} - I_D}{I_D^{\text{apb}}} .$$

PROTOCOL 4

Measuring FRET by Sensitized Emission

This protocol describes the steps involved for a sensitized emission measurement and analysis. The considerations described in Protocol 3 concerning image acquisition and analysis also apply here.

MATERIALS

Equipment

The equipment required is the same as in Protocol 3 with the addition of a FRET-filter set, which allows excitation of the donor and collection of acceptor fluorescence.

METHOD

1. Characterize the bleed-through (B) and direct-excitation (C) factors. This needs to be done only once, either at the beginning or at the end of the experiment.
 - i. Acquire an image of a sample with donor-tagged molecules *only* (either by choosing a cell without an acceptor or by removing the acceptor by photobleaching) using the FRET-filter set ($I_{DA}^{\text{only donor}}$). Acquire an image of the same sample, using the donor-filter set ($I_D^{\text{only donor}}$). Using the background-corrected and thresholded images, calculate B as

$$B = \frac{\langle I_{DA}^{\text{only donor}} \rangle}{\langle I_D^{\text{only donor}} \rangle} .$$

Note that the result is a scalar because the mean value ($\langle \rangle$) of the images is calculated, and this is used in both the numerator and the denominator.

- ii. Acquire an image of a sample with acceptor-tagged molecules *only* using the FRET-filter set ($I_{DA}^{\text{only acceptor}}$). Acquire an image of the same sample, using the acceptor-filter set ($I_A^{\text{only acceptor}}$). Using the background-corrected and thresholded images, calculate C as

$$C = \frac{\langle I_{DA}^{\text{only acceptor}} \rangle}{\langle I_A^{\text{only acceptor}} \rangle} .$$

2. Select a cell that contains donor and acceptor fluorescence.
3. Acquire an image with the donor-filter set (I_D).
4. Acquire an image with the FRET-filter set (I_{DA}).
5. Acquire an image with the acceptor-filter set (I_A).
6. Calculate the sensitized emission I_{SENS} using the scalar correction factors (B and C) and the images (I_D , I_{DA} , and I_A) corrected for background:

$$I_{\text{SENS}} = I_{DA} - B \cdot I_D - C \cdot I_A .$$

7. Calculate the apparent energy-transfer efficiency in each pixel:

$$AFE_A = \frac{I_{DA} - B \cdot I_D - C \cdot I_A}{I_A} = \frac{I_{\text{SENS}}}{I_A} .$$

► PROTOCOL 5

Measuring FRET by Confocal Time-Correlated Single-Photon Counting Fluorescence Lifetime Imaging

This protocol describes the steps involved for measuring FRET by fluorescence lifetime imaging (FLIM) using confocal time-correlated single-photon counting (TCSPC). The considerations described in Protocol 3 concerning image acquisition and analysis also apply here. TCSPC data can be fitted to a decay function with the software provided by the manufacturer of the fluorescence lifetime module. Measured data of the the phosphorylation of the EGFR using this technique are shown in Figure 4.

MATERIALS

Equipment

Confocal microscope equipped with a fluorescence lifetime module (e.g., from PicoQuant or Becker & Hickl)

This module usually contains a high repetition rate (10–80 MHz) pulsed (100-psec) laser, an avalanche photodiode (APD) configured for single-photon detection or fast photomultiplier tubes, and the electronics to time the arrival photons with picosecond resolution. All devices are synchronized to the scanning of the confocal microscope in such a way that each photon can be assigned to a pixel in the image.

Neutral density-filter set and a mirror-scattering sample (for measuring the instrument response function [IRF]; optional)

METHOD

1. (*Optional*) Characterize the IRF of the system for deconvolution of the decay profile.
 - i. Put a mirror in the sample plane.
 - ii. Put a neutral density filter (typically optical density 3) in the detection path.
 - iii. Focus in the mirror.

Caution: APDs are very sensitive to light. Typical saturation values are around 10^6 cps.
 - iv. Take a FLIM image containing a total of 10^6 photons.

Caution: High-count rates lead to artifacts because of pulse pileup. Low count rate leads to bad signal-to-noise ratios. For imaging, keep the count rate at 1%–10% of the saturation value.
 - v. Bin the complete image to obtain an arrival-time histogram. The shape is usually a non-symmetrical pulse of 100–400 psec FWHM (full width at half-maximum). Save it as the IRF.

Shorter pulses lead to better resolution of the fluorescence decay profile. Most laser diodes achieve shorter pulses when the power is set at low values.
2. (*Optional*) Acquire a fluorescence image with the acceptor-filter set (I_A) to document the distribution of the acceptor.
3. Characterize the fluorescence decay profile of the donor. This needs to be done once, either at the beginning or at the end of the experiment.

- i. Acquire an image of a sample with donor-tagged molecules *only* (either by choosing a cell without an acceptor or by removing an acceptor by photobleaching).

Caution: Because EGFR is expressed strongly in the plasma membrane, the fluorescence can be much higher in those pixels leading to a local pulse pile-up artifact. Most systems display the count rate averaged over a certain time. Keeping a slow scan speed will allow you to have a local representative figure of the count rate.
- ii. Bin the complete image to obtain the arrival time histogram of the donor.
- iii. Fit the data with a single exponential decay function. The decay constant (τ_D) should be ~ 2.5 nsec for EGFP and ~ 3 nsec for EYFP. If the IRF has been measured, a full reconvolution fit can be performed. On the contrary, data should be tail fitted by selecting only the last part of the decay.
- iv. In addition to the parameters, the software algorithm will provide two evaluations of the quality of the fit: (a) the residuals of the fit, which should be homogeneously distributed around 0, and (b) the reduced χ^2 , which is the sum of the squared residuals normalized by the number of degrees of freedom (number of points minus the number of parameters). This value should be close to 1 for TCSPC data.
- v. Repeat for more cells, and calculate the mean value to obtain a more robust determination.
4. Acquire a FLIM image of the donor in the presence of the acceptor with the donor filter following the recommendations of Step 1.
 - i. Bin the complete image I_D to obtain the decay profile of the donor in the presence of the acceptor.
 - ii. Fit the decay profile using a double exponential decay function, where one of the decay constants (τ_D) is fixed to the fluorescence lifetime obtained in Step 3iii and the other is left free to be fitted (τ_F).
5. Calculate the FRET efficiency using Equation 7.
6. Calculate the mean value of α using Equation 6.
7. (*Optional*) Fit a double exponential decay fixing the values obtained for τ_D and τ_F , and let α be fitted freely pixel by pixel using the same equation as in the previous step.

A maximum-likelihood algorithm is suggested when the counts per bin are less than 10, as the usual χ^2 minimization yields biased results.

The FRET efficiency is only dependent on the donor–acceptor pair, and thus it should be constant across all data sets. A better approach to fit the data is to perform a global analysis. In this method, all data sets are fitted simultaneously, linking the values for τ_D and τ_F . This tightens the χ^2 space and leads to a more robust determination of the parameters (Lakowicz 2006).

► PROTOCOL 6

Measuring Protein Interaction by FCCS

This protocol describes the steps involved for measuring protein interactions by FCCS using a confocal microscope.

MATERIALS

Reagents

Labeling selection

Molecular brightness is the first selection criterion for FCCS experiments because it determines the signal-to-noise ratio. Blinking and pH sensitivity should be avoided where possible. Spectral separation between the fluorophores is important to reduce cross talk between channels. Chemical dyes such as the Alexa and Cy families are bright, photostable, and available in many different wavelengths. Having the advantage of being genetically encoded, fluorescent proteins (FPs) can be used, even though their brightness and photostability are not comparable with chemical dyes. The EGFP and mCherry (red) have been shown to be an appropriate pair for FCCS. However, the data have to be corrected for the slow maturation rate of the red FP, which yields a dark population. New red variants with faster maturation such as mKate or mKate2 might be good alternatives. Cyan fluorescent protein (CFP) in a pair with EYFP has also been used successfully for FCCS. Nevertheless, new and more photostable FPs such as monomeric teal FP (mTFP) and monomeric citrine (mCitrine) should be favored.

Sample

Literature for FCCS describes several examples that have been studied, including the interaction between c-Jun and c-Fos22 (Baudendistel et al. 2005), the interaction among the MAPKs Ste11, Ste7, and Fus3 and the scaffold protein Ste5 in yeast pheromone signaling (Maeder et al. 2007), and the interaction between different subunits of the bacterial cholera toxin along the endocytic pathway (Bacia et al. 2002). It is important to have a negative control (no interaction or low affinity) and a positive control (constituted interaction or strong affinity).

Sample labeling

It is essential to avoid dark molecules (such as unlabeled or immature fluorescent protein) and any free dye as this will bias the result.

Equipment

Confocal microscope equipped with a FCCS module (such as Zeiss ConfoCor 3 or Leica FCS2) that contains two single-photon-counting avalanche photodiodes

High numerical aperture, water-immersion objective with chromatic correction to maximize the volume overlap between the different wavelengths

An objective equipped with a correction collar is important to adapt for different glass thicknesses.

METHOD

Initial Setup

1. Pinhole alignment: Using a solution of dye, change the position of the pinhole(s) to maximize the intensity in the detector. Do this by iteratively maximizing in the lateral and axial directions.

2. Make sure that the water used for immersion and all solutions are nonfluorescent by measuring them without the sample. The count rate should be less than 300 Hz.
3. Obtain the structural parameter of your system by measuring the autocorrelation of a dye in solution with known concentration and diffusion time. The length of the acquisition and number of repetitions depend on the signal-to-noise ratio. Ten repetitions of 10 sec each is usually a good choice. Discard measurements with aggregates as evidenced from an abnormal increase in the intensity trace.
4. Using a FCCS calibration sample, check that the detection volumes for the different channels overlap. The dwell time in the confocal volume should be the same in both channels. The cross-correlation curve should not present signs of blinking.
5. Determine the optimal laser to be used in the actual experiment. Using single fluorescent-labeled samples, measure the diffusion time as a function of the laser power. The effect of photobleaching will be evidenced by the decrease in the dwell time. Where possible, avoid photobleaching while keeping the counts per molecule between 1 kHz and 5 kHz (determined by dividing the count rate by the number of molecules N in the volume element).

Measurement

6. If reverse-transfected cells are used, select a cell with moderate-to-low expression level.
7. For the sample and the controls, measure for 10 sec, and repeat 10 times. Repeat, if a significant number of intensity traces present strong intensity jumps.
8. Select the traces that show a homogenous intensity trace and do not exhibit strong bleaching. Compute the autocorrelation, and fit it using the appropriate model.
9. Compute the cross-correlation, and determine the concentration of protein complex using the cross-autocorrelation amplitudes (see Equation 10).

RECIPES

CAUTION: See Appendix for proper handling of materials marked with <!.>.

DMF; dry <!.>

DMF is dried by adding approximately one-third volume of hygroscopic resin to the storage vessel. For example, AG 501-X8 mixed bed resin (from Bio-Rad Laboratories) can be placed permanently in the DMF stock bottle. If there is any doubt as to the integrity of the DMF, either add further fresh resin or replace old resin with fresh resin. This issue is a consideration when problems arise during labeling of proteins to a desired ratio. Water in the labeling reaction (potentially from the DMF) will compete for the reaction with free dye.

PBS

Reagent	Quantity	Final concentration
NaCl	8 g	137 mM
KCl <!.>	0.2 g	2.7 mM
Na ₂ HPO ₄	1.44 g	10 mM
KH ₂ PO ₄	0.24 g	1.8 mM

If necessary, PBS may be supplemented with the following:

Reagent	Quantity	Final concentration
CaCl ₂ •2H ₂ O	0.133 g	1 mM
MgCl ₂ •6H ₂ O	0.10 g	0.5 mM

PBS can be made as a 1X solution or a 10X stock. To prepare 1 L of 1X solution, dissolve the reagents listed above in 800 mL of H₂O. Adjust the pH to 7.4 (or 7.2, if required) with HCl, and then add H₂O to 1 L. Dispense the solution into aliquots, and sterilize them by autoclaving for 20 min at 15 psi (1.05 kg/cm²) on liquid cycle or by filter sterilization. Store at room temperature. To prepare a 10X stock, dissolve 80 g of NaCl, 2 g of KCl, 14.4 g of Na₂HPO₄, and 2.4 g of KH₂PO₄ in 1 L of distilled, deionized water.

Tris-Cl (100 mM; pH 8.0)

To prepare a 1-M solution, dissolve 121.1 g of Tris base in 800 mL of H₂O. Adjust the pH to the desired value by adding concentrated HCl <!\>.

pH	HCl
7.4	70 mL
7.6	60 mL
8.0	42 mL

Allow the solution to cool to room temperature before making final adjustments to the pH. Adjust the volume of the solution to 1 L with H₂O. Dispense into aliquots, and sterilize by autoclaving. If the 1-M solution has a yellow color, discard it, and obtain Tris of better quality. The pH of Tris solutions is temperature dependent and decreases ~0.03 pH units for each 1°C increase in temperature. For example, a 0.05-M solution has pH values of 9.5, 8.9, and 8.6 at 5°C, 25°C, and 37°C, respectively.

Activated Sodium Orthovanadate <!\>

Reagent	Quantity	Final concentration
Sodium orthovanadate <!\>	0.732 g	200 mM

Dissolve sodium orthovanadate (Sigma #S6508) in 18 mL water, and adjust the pH to 10.0 with 1 M NaOH or 1 M HCl <!\> (the starting pH varies depending on the lot of the chemical; at pH 10.0 the solution is a yellow color). Boil the solution until colorless (~10 min), and then cool to room temperature. Readjust the pH to 10.0 and repeat boiling and cooling until the solution remains colorless and the pH stabilizes at 10.0. Adjust the final volume to 20 mL with water and store in aliquots at -20°C. (See Gordon 1991.)

Mowiol Mounting Medium

This is the desired mounting medium as it does not quench GFP fluorescence. Mix 6 mL of glycerol, 2.4 g of Mowiol 4-88 (Calbiochem), and 6 mL of distilled, deionized water. Shake for 2 h at room temperature. Add 12 mL of 200 mM Tris-HCl (pH 8.5), and incubate at 50°C with occasional mixing until the Mowiol dissolves (~3 h). Filter through a 0.45-µm membrane filter, and store in aliquots at 4°C for weeks or at -20°C for months.

Paraformaldehyde Fixative Solution (4%) <!\>

Dissolve 4 g of paraformaldehyde <!\> (Sigma-Aldrich) in 50 mL of distilled, deionized water, and then add 1 mL of 1 M NaOH solution. Stir gently on a heating block (~65°C) until the

paraformaldehyde is dissolved. Then add 10 mL of 10× PBS, and cool to room temperature. Adjust the pH to 7.4 with 1 M HCl (~1 mL), and then adjust the final volume to 100 mL with distilled, deionized water. Filter the solution through a 0.45- μ m membrane filter to remove any particulate matter, and store in aliquots at -20°C for several months. Avoid repeated freeze–thawing of the paraformaldehyde solution.

REFERENCES

- Bacia K, Majoul IV, Schwille P. 2002. Probing the endocytic pathway in live cells using dual-color fluorescence cross-correlation analysis. *Biophys J* **83**: 1184–1193.
- Bacia K, Kim SA, Schwille P. 2006. Fluorescence cross-correlation spectroscopy in living cells. *Nat Methods* **3**: 83–89.
- Bastiaens PIH, Jovin TM. 1996. Microspectroscopic imaging tracks the intracellular processing of a signal transduction protein: Fluorescent-labeled protein kinase C β I. *Proc Natl Acad Sci* **93**: 8407–8412.
- Bastiaens PIH, Squire A. 1999. Fluorescence lifetime imaging microscopy: Spatial resolution of biochemical processes in the cell. *Trends Cell Biol* **9**: 48–52.
- Baudendistel N, Muller G, Waldeck W, Angel P, Langowski J. 2005. Two-hybrid fluorescence cross-correlation spectroscopy detects protein–protein interactions in vivo. *ChemPhysChem* **6**: 984–990.
- Betzig E, Patterson GH, Sougrat R, Lindwasser OW, Olenych S, Bonifacino JS, Davidson MW, Lippincott-Schwartz J, Hess HF. 2006. Imaging intracellular fluorescent proteins at nanometer resolution. *Science* **313**: 1642–1645.
- Bolte S, Cordelieres FP. 2006. A guided tour into subcellular colocalization analysis in light microscopy. *J Microsc* **224**: 213–232.
- Brown CM, Dalal RB, Hebert B, Digman MA, Horwitz AR, Gratton E. 2008. Raster image correlation spectroscopy (RICS) for measuring fast protein dynamics and concentrations with a commercial laser scanning confocal microscope. *J Microsc* **229**: 78–91.
- Csete ME, Doyle JC. 2002. Reverse engineering of biological complexity. *Science* **295**: 1664–1669.
- Dowling K, Dayel MJ, Lever MJ, French PMW, Hares JD, Dymoke-Bradshaw AKL. 1998. Fluorescence lifetime imaging with picosecond resolution for biomedical applications. *Opt Lett* **23**: 810–812.
- Forster T. 1948. Zwischenmolekulare energiewanderung und fluoreszenz. *Ann Phys* **2**: 55–75.
- French AP, Mills S, Swarup R, Bennett MJ, Pridmore TP. 2008. Colocalization of fluorescent markers in confocal microscope images of plant cells. *Nat Protoc* **3**: 619–628.
- Gadella TWJ, Jovin TM, Clegg RM. 1993. Fluorescence lifetime imaging microscopy (FLIM)—Spatial-resolution of microstructures on the nanosecond time-scale. *Biophys Chem* **48**: 221–239.
- Giepmans BNG, Adams SR, Ellisman MH, Tsien RY. 2006. Review—The fluorescent toolbox for assessing protein location and function. *Science* **312**: 217–224.
- Gordon JA. 1991. Use of vanadate as protein-phosphotyrosine phosphatase inhibitor. *Methods Enzymol* **201**: 477–482.
- Haj FG, Verveer PJ, Squire A, Neel BG, Bastiaens PIH. 2002. Imaging sites of receptor dephosphorylation by PTP1B on the surface of the endoplasmic reticulum. *Science* **295**: 1708–1711.
- Haustein E, Schwille P. 2007. Fluorescence correlation spectroscopy: Novel variations of an established technique. *Annu Rev Biophys Biomol Struct* **36**: 151–169.
- Hein B, Willig KI, Hell SW. 2008. Stimulated emission depletion (STED) nanoscopy of a fluorescent protein-labeled organelle inside a living cell. *Proc Natl Acad Sci* **105**: 14271–14276.
- Heintzmann R, Ficz G. 2007. Breaking the resolution limit in light microscopy. *Method Cell Biol* **81**: 561–580.
- Kholodenko BN. 2006. Cell-signalling dynamics in time and space. *Nat Rev Mol Cell Biol* **7**: 165–176.
- Kim SA, Heinze KG, Schwille P. 2007. Fluorescence correlation spectroscopy in living cells. *Nat Methods* **4**: 963–973.
- Lakowicz JR. 2006. *Principles of fluorescence spectroscopy*, 3rd ed. Springer, New York.
- Lakowicz JR, Berndt KW. 1991. Lifetime-selective fluorescence imaging using an Rf phase-sensitive camera. *Rev Sci Instrum* **62**: 1727–1734.
- Lakowicz JR, Cherek H, Gryczynski I, Joshi N, Johnson ML. 1987. Analysis of fluorescence decay kinetics measured in the frequency-domain using distributions of decay times. *Biophys Chem* **28**: 35–50.
- Maeder CI, Hink MA, Kinkhabwala A, Mayr R, Bastiaens PI, Knop M. 2007. Spatial regulation of Fus3 MAP kinase activity through a reaction-diffusion mechanism in yeast pheromone signalling. *Nat Cell Biol* **9**: 1319–1326.
- Magde D, Webb WW, Elson E. 1972. Thermodynamic fluctuations in a reacting system—Measurement by fluorescence correlation spectroscopy. *Phys Rev Lett* **29**: 705–708.
- Mahajan NP, Linder K, Berry G, Gordon GW, Heim R, Herman B. 1998. Bcl-2 and Bax interactions in mitochondria probed with green fluorescent protein and fluorescence resonance energy transfer. *Nat Biotechnol* **16**: 547–552.
- Medda R, Bewersdorf J, Hell SW. 2007. 4Pi microscopy of quantum dot-labeled cellular structures. *Eur J Cell Biol* **86**: 62.
- Milo R, Shen-Orr S, Itzkovitz S, Kashtan N, Chklovskii D, Alon U. 2002. Network motifs: Simple building blocks of complex networks. *Science* **298**: 824–827.
- Patterson GH, Piston DW, Barisas BG. 2000. Forster distances between green fluorescent protein pairs. *Anal Biochem* **284**: 438–440.
- Pieroni E, Van Bentem SD, Mancosu G, Capobianco E, Hirt H, de la Fuente A. 2008. Protein networking: Insights into global functional organization of proteomes. *Proteomics* **8**: 799–816.
- Sanchez SA, Gratton E. 2005. Lipid-protein interactions revealed by two-photon microscopy and fluorescence correlation spectroscopy. *Acc Chem Res* **38**: 469–477.
- Santos SDM, Verveer PJ, Bastiaens PIH. 2007. Growth factor-induced MAPK network topology shapes Erk response determining PC-12 cell fate. *Nat Cell Biol* **9**: 324–330.
- Sheffield JB. 2007. ImageJ, a useful tool for biological image processing and analysis. *Microsc Microanal* **13**: 200–201.
- Tyson JJ, Chen KC, Novak B. 2003. Sniffers, buzzers, toggles and blinkers: Dynamics of regulatory and signaling pathways in the cell. *Curr Opin Cell Biol* **15**: 221–231.
- Verveer PJ, Bastiaens PIH. 2008. Quantitative microscopy and systems biology: Seeing the whole picture. *Histochem Cell Biol* **130**: 833–843.
- Verveer PJ, Wouters FS, Reynolds AR, Bastiaens PIH. 2000. Quantitative imaging of lateral ErbB1 receptor signal propagation in the plasma membrane. *Science* **290**: 1567–1570.
- Wouters FS, Verveer PJ, Bastiaens PIH. 2001. Imaging biochemistry inside cells. *Trends Cell Biol* **11**: 203–211.
- Zamir E, Bastiaens PIH. 2008. Reverse engineering intracellular biochemical networks. *Nat Chem Biol* **4**: 643–647.
- Zhu XW, Gerstein M, Snyder M. 2007. Getting connected: Analysis and principles of biological networks. *Gene Dev* **21**: 1010–1024.

